Analytica Chimica Acta 686 (2011) 81–86

Contents lists available at ScienceDirect

Analytica Chimica Acta

journal homepage: www.elsevier.com/locate/aca

Magnetic loading of tyrosinase-Fe_3O_4/mesoporous silica core/shell microspheres for high sensitive electrochemical biosensing

Shuo Wu*, Hainan Wang, Shengyang Tao*, Chan Wang, Lihui Zhang, Zhiguang Liu, Changgong Meng

School of Chemistry, Dalian University of Technology, Dalian 116023, PR China

ARTICLE INFO

Article history:
Received 20 September 2010
Received in revised form
27 November 2010
Accepted 30 November 2010
Available online 8 December 2010

Keywords:
Tyrosinase
Fe_3O_4/$mSiO_2$ core/shell mesoporous microspheres
Magnetic loading
Flow injection analysis
Amperometry

ABSTRACT

A new protocol is proposed for magnetic loading and sensitive electrochemical detection of phenol via the tyrosinase cross-linked mesoporous magnetic core/shell microspheres. The mesoporous magnetic microspheres, characterized by transmission electron microscopy, N_2 adsorption/desorption isotherms, and magnetic curve displays high capacity for enzyme immobilization and strong magnetism to adhere to the magnetic electrode surface without any additional adhesive reagent. The biosensor exhibits a wide linear response to phenol ranging from 1.0×10^{-9} to 1.0×10^{-5} M, a high sensitivity of 78 μA mM^{-1}, a low detection limit of 1 nM, and a fast response rate (less than 5 s). The proposed method is simple, rapid, inexpensive and convenient in electrode renewal, which is recommended as a promising experimental platform for wider applications in biosensing.

1. Introduction

Electrochemical biosensors show great potential in clinical, industrial, and environmental monitoring due to their inherent properties of high sensitivity, low cost and portability. Fabrication of the bio-functional interface on the solid electrode surface is a crucial step for the design of a biosensor, which requires a well maintained high activity of the biomolecule, fast electron transfer kinetics, low diffusion limitation, high stability and renewable transducer surface [1–3]. Therefore, many strategies including direct physical adsorption [4], covalent cross-linking [5,6], electrodeposition [7,8], layer-by-layer assembly [9,10] and encapsulation [11,12] have been employed to fabricate those bio-interfaces. However, some of these methods suffer from problems of poor stability, decreased enzyme activity, or difficult renewal ability. Thus, searching for a simple, renewable, and reliable scheme to fabricate the bio-functional interface is of considerable interest.

Magnetic loading [13–19], a recently emerged bio-interface fabrication protocol with the help of external magnetic field, is proposed as an excellent choice for biosensing. During the last five years, several kinds of magnetic nanomaterials including Fe_2O_3 filled carbon nanotubes [13], iron oxide nanoparticles [14], $MgFe_2O_4$/SiO_2 nanocomposite [15], cationic magnetic beads [16], magnetized silica-based microparticle [17], magnetic polymeric nanocomposites [18], and carbon nanotube/nano-Fe_3O_4 composite [19] have been used for the fabrication of magnetic loaded biosystems. These studies indicate that the magnetic nanomaterials based magnetic loading protocol could controllable fix/detach the nanomaterial/biomolecule nanocomposite on/off the magnetic electrode, reduce the analytes diffusion limitation, and well maintain the activity of enzyme, thus show great perspective for biosensor fabrication.

Magnetic mesoporous material, one type of magnetic nanomaterials have been widely used in bioseparation [20] and biocatalysis [21,22], which shows great prospective in enzyme activity maintenance, substrate preconcentration, and magnetic loading due to their good properties of acceptable magnetism, high versatility in surface modification, and large surface areas. The introduction of those magnetic mesoporous material in enzyme immobilization for biosensing may open up a new avenue to achieve high sensitive, fast response, and magnetically control. However, there were barely reports in this area. Although a magnetic mesocellular carbon foam was synthesized in 2005 by Hyeon and co-workers [23] for the glucose oxidase immobilization and magnetically switchable bioelectrocatalysis, there was no further application for biosensing.

Herein, a new Fe_3O_4 core/mesoporous silica shell magnetic mesoporous microspheres (Fe_3O_4/$mSiO_2$) was introduced for the design of novel magnetically loaded biosensor. Tyrosinase (Tyr),

* Corresponding authors. Tel.: +86 411 84706293.
E-mail address: wushuo@dlut.edu.cn (S. Wu).

0003-2670/$ – see front matter © 2010 Elsevier B.V. All rights reserved.
doi:10.1016/j.aca.2010.11.053

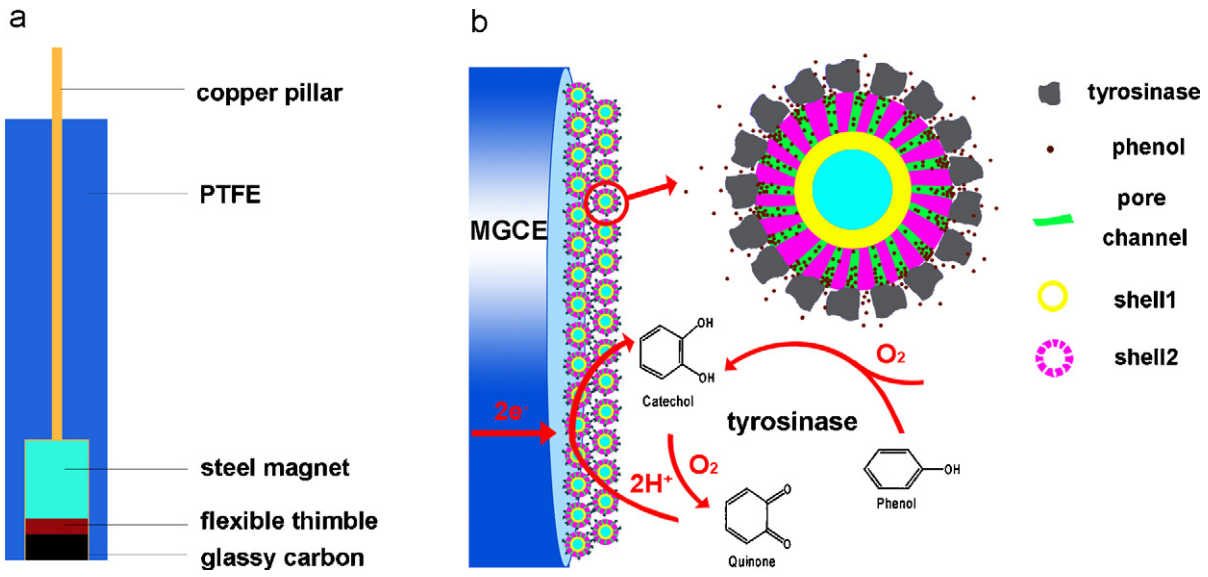

Fig. 1. The diagram of the magnetic glassy carbon electrode (a) and the working scheme of the biosensor (b).

a phenoloxidase that could catalyze the transformation of a large number of phenolic compounds, was cross-linked to the aldehyde group modified Fe_3O_4@$m$$SiO_2$ (Tyr-Fe_3O_4@$m$$SiO_2$) and used as a model for the fabrication of a magnetic loaded biosensor. Combining with magnetic interaction and flow injection analysis (FIA), an automated magnetically controllable phenol biosensor was fabricated. The proposed biosensor showed high sensitivity, low limit of detection, wide linear range, fast response, good stability, and easy renewal ability, indicating that Fe_3O_4@$m$$SiO_2$ could provide a novel platform for biofunctional interface fabrication and biosensing application.

2. Experimental

2.1. Materials

Tyr (from mushroom, EC 1.14.18.1, 3933 units mg^{-1}) was obtained from Sigma. All other reagents (analytical grade) were purchased from Beijing Chemical Reagents Company, and used without further purification. Doubly distilled water was used in all experiments. Sea water from Bohai Sea, Dalian was used for the practical sample analysis.

2.2. Instrumentation

The nitrogen adsorption and desorption isotherms were measured at 77 K using an ASAP 2010 analyzer (Micromeritics Co. Ltd.). Before measurement, samples were degassed under vacuum at 373 K for 4 h. Transmission electron microscopy (JEOL, JEM-2010) was performed to study the morphology and particle size of the samples. Magnetic characterization was carried out using a VSM with fields up to 10,000 Oe and at a temperature of 300 K. Electrochemical measurements were performed on a CHI 1130 (CH Instrument Co., Shanghai) electrochemical analyzer with a conventional three-electrode system with a homemade Ag/AgCl electrode as a reference electrode, a platinum silk with 0.5 mM diameter as a counter electrode, and a modified magnetic glassy carbon electrode (MGCE) as a working electrode. The magnetically controlled biosensor was connected to the flow injection system comprised of a peristaltic pump (BT100-1J, Baoding Longer Precision Pump Co. Ltd., Baoding, China), a six-port injection valve and a homemade poly(methyl methacrylate) flow cell with volume of 200 μL. All electrochemical experiments were carried out at room temperature in air-saturated 0.1 M PBS solution (pH 6.0). The flow rate was 2.0 mL min^{-1}.

2.3. Fabrication of Fe_3O_4@$m$$SiO_2$ and Fe_3O_4@SiO_2

The Fe_3O_4@$m$$SiO_2$ mesoporous microspheres and microspheres with nonporous silica coating (Fe_3O_4@SiO_2) were prepared according to the previously reported method [24]. First, Fe_3O_4 nanoparticles were prepared by adding 1.35 g $FeCl_3{\cdot}6H_2O$, 3.60 g anhydrous sodium acetate, and 1.00 g polyethylene glycol in 40 mL ethylene glycol, followed by 30 min vigorously stirring at room temperature and 8 h solvothermal treatment at 200 °C. 0.5 g of the obtained Fe_3O_4 nanoparticles were treated with 0.1 M HCl aqueous solution by ultrasonication for 10 min. Then the nanoparticles were dispersed in a mixture containing 80 mL ethanol, 20 mL deionized water and 1.0 mL concentrated ammonia and homogenized for 0.5 h to form a uniform dispersion, then, 0.03 g ethyl orthosilicate (TEOS) was added into the mixture and stirred at room temperature for 6 h. Subsequently, the resulted microspheres were dispersed in a mixed solution containing 0.30 g cetyltrimethylammonium bromide, 80 mL doubly distilled water, 1.00 g concentrated ammonia, and 60 mL ethanol and homogenized for 0.5 h to form a uniform dispersion, then 0.40 g TEOS was added dropwise to the dispersion with continuous stirring for 6 h to get the Fe_3O_4@$m$$SiO_2$. At last, 1.00 g of the obtained product was dispersed in ethanol solution containing 2% NH_4NO_3 and stirred at 60 °C for 15 min to remove the surfactant.

2.4. Fabrication of Try conjugated magnetic nanocomposite

The obtained Fe_3O_4@SiO_2 and Fe_3O_4@$m$$SiO_2$ were respectively grafted with amino groups by refluxing 0.1 g of the materials in 100 °C toluene solution containing 1% 3-aminopropyltriethoxysilane for 12 h. Subsequently, 4.0 mg of the amino functionalized materials were dispersed in 1.0 mL phosphate buffer solution (PBS) (0.1 M, pH = 7.0) containing 2.5% glutaraldehyde and stirred for 3 h. At last, the aldehyde grafted microspheres were separated by magnet and redispersed in 0.8 mL PBS (pH = 7.0) containing 0.4 mg mL^{-1} Tyr and left to react at 4 °C for 48 h with occasionally stirring. The resulted Tyr conjugated magnetic materials were denoted as Tyr-Fe_3O_4@$m$$SiO_2$ and Tyr-Fe_3O_4@SiO_2, respectively.

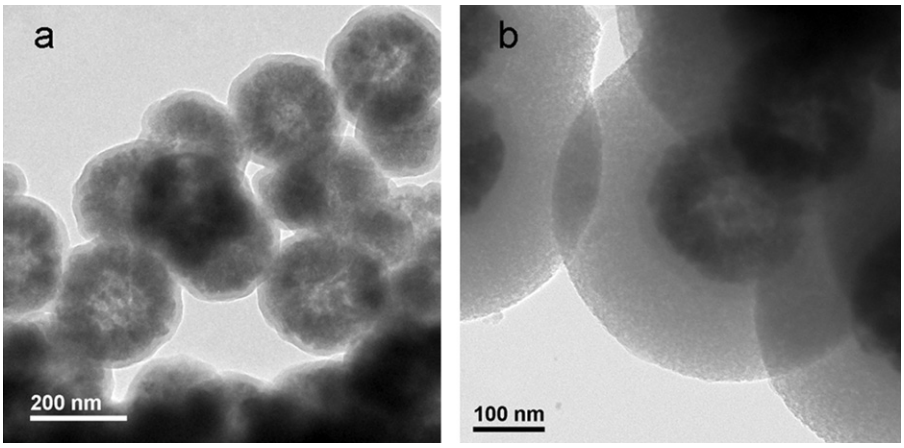

Fig. 2. TEM images of the Fe_3O_4@SiO_2 (a) and the Fe_3O_4@$mSiO_2$ (b).

2.5. Preparation of the magnetic loaded phenol biosensor

MGCE (3 mm in diameter) was purchased from Jiangfen Instruments, Inc., China. The inner structure of the electrode was shown in Fig. 1a. The MGCE was firstly polished to a mirror finish with 0.3 and 0.05 μm alumina slurry followed by thoroughly rinsing with deionized water. After sonicating successively in 1:1 nitric acid, acetone and ethanol, the electrodes were rinsed with deionized water and dried at room temperature. The Tyr-Fe_3O_4@$mSiO_2$ modified electrode (Tyr-Fe_3O_4@$mSiO_2$/MGCE) was fabricated by dropping 3 μL of the 0.5 mg mL^{-1} Tyr-Fe_3O_4@$mSiO_2$ suspension on the surface of the MGCE and followed with water evaporation. For comparison, the Tyr-Fe_3O_4@SiO_2/MGCE and the (Tyr-Fe_3O_4@$mSiO_2$)-PVA/GMCE obtained by further coating of 3 μL of 2% PVA on the Tyr-Fe_3O_4@$mSiO_2$/MGCE were prepared. The modification and working scheme of the biosensor was shown in Fig. 1b.

3. Results and discussion

3.1. Characterization of the core–shell magnetic nanoparticles

The coating of silica shell on the magnetic core could provide the magnetic materials with easier functionalizable surface and prevent them from aggregation. Fig. 2a and b show the TEM images of Fe_3O_4@SiO_2 and Fe_3O_4@$mSiO_2$. A thin and dense silica layer could be observed on the Fe_3O_4 outer surface, which is about 25 nm thick. After further coating of mesoporous silica on the surface of Fe_3O_4@SiO_2, a three layer structure with a looser layer outside is obviously observed, correspondingly, the particle size of the Fe_3O_4@$mSiO_2$ has increased to about 450 nm, which is about 150 nm larger than that of the Fe_3O_4@SiO_2. The porous nature of the Fe_3O_4@$mSiO_2$ is also proved by the N_2 adsorption/desorption experiment (Fig. 3a), which exhibits typical IV isotherms. The pore size is 2.5 nm calculated from the desorption branch of the nitrogen isotherm with BJH (Barrett–Joyner–Halenda) model (Fig. 3b), indicating a uniform mesostructure. The porous structure increases the surface roughness, which facilitates the immobilization of enzyme by increasing amount and better maintaining the enzyme activity. Fig. 3c shows the magnetization curve of Fe_3O_4@$mSiO_2$, no hysteresis loop and no remanence was detected, suggesting the magnetic nanocomposites composed of many small superparamagnetic particles still maintained the superparamagnetic property. With superparamagnetism, the Fe_3O_4@$mSiO_2$ microsphere could be well re-dispersed in the solution thus was beneficial for the recycle usage. The saturation magnetization of Fe_3O_4@$mSiO_2$ is 27.5 emu g^{-1} (Fig. 3c), which is much larger than that of the magnetic mesocellular foam [23]. As we know, the stability of magnetic nanocomposite on the magnetic electrode surface depends on four factors, the physical adsorption and magnetic interaction, which facilitate the adhesion of the magnetic nanocomposite, and gravity

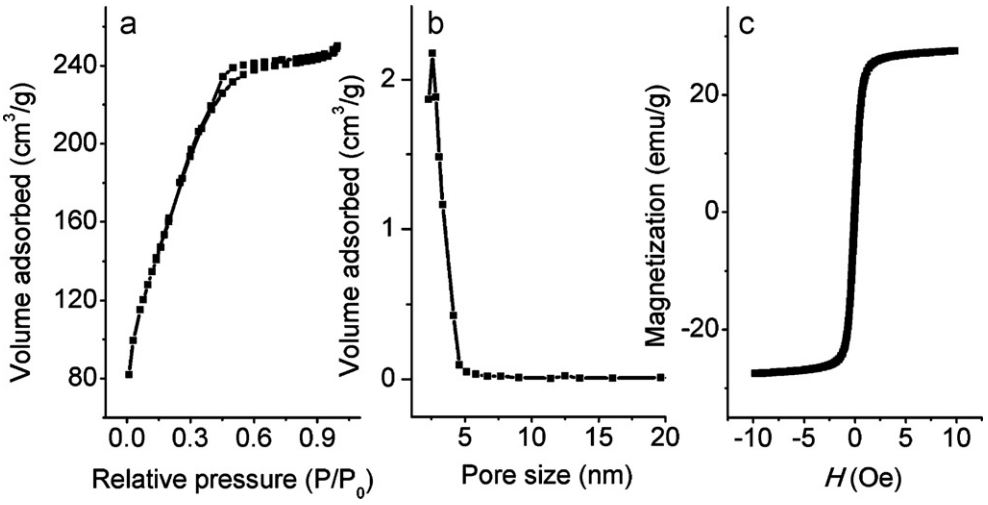

Fig. 3. Nitrogen sorption isotherms (a), pore size distribution (b), and magnetic curve of the Fe_3O_4@$mSiO_2$ (c).

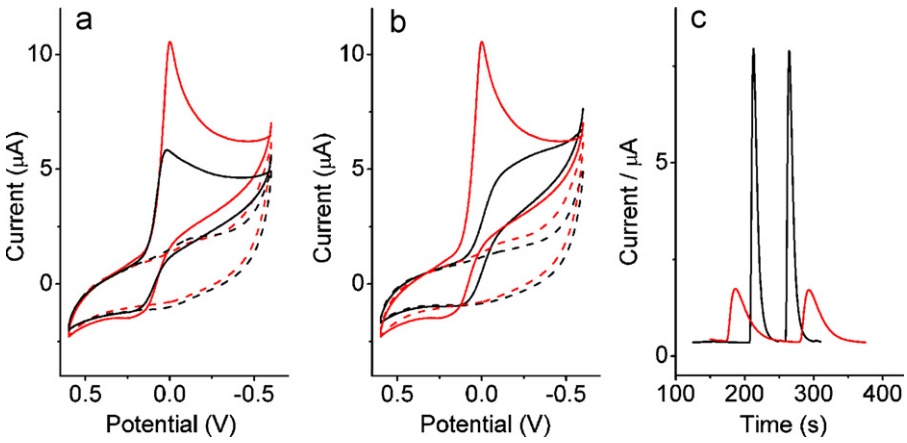

Fig. 4. (a) CVs of the Tyr-Fe_3O_4@SiO_2/MGCE (black) and the Tyr-Fe_3O_4@$mSiO_2$/MGCE (red) with (solid line) and without (dash line) the addition of 50 μM phenol in 0.1 M PBS 6.0 at 50 mV s^{-1}, (b) CVs of Tyr-Fe_3O_4@$mSiO_2$/MGCE (red) and (Tyr-Fe_3O_4@$mSiO_2$)-PVA/MGCE (black) with (solid line) and without (dash line) 50 μM phenol in 0.1 M PBS 6.0 at 50 mV s^{-1}, and (c) the flow injection amperometric response of the Tyr-Fe_3O_4@$mSiO_2$/MGCE (black) and (Tyr-Fe_3O_4@$mSiO_2$)-PVA/MGCE (red) to 10 μM phenol at −0.15 V. (For interpretation of the references to color in this figure legend, the reader is referred to the web version of the article.)

and washing force, which may cause the detachment of it. The physical adsorption could be improved by decreasing the particle size (450 nm in this case) to enhance the surface area. And the saturation magnetism of the nanoparticles (27.5 emu g^{-1}) is adequate for the stable magnetic interaction. The combination of strong physical and magnetic interations make the magnetic nanocomposite sustained on the electrode surface under the flow through conditions.

3.2. Electrochemical performance of the biosensor

Fig. 4a shows the cyclic voltammograms (CVs) of the Tyr-Fe_3O_4@SiO_2/MGCE and the Tyr-Fe_3O_4/$mSiO_2$/MGCE in 0.1 M air saturated pH 6.0 PBS with and without the addition of 50 μM phenol. Without addition of phenol, only low background currents were observed. Upon the addition of phenol to the buffer solution, the CVs of Tyr-Fe_3O_4@SiO_2/MGCE and the Tyr-Fe_3O_4@$mSiO_2$/MGCE both gave peak shaped catalytic reduction waves, which were caused by the reduction of quinone species liberated from the enzymatic reaction of Tyr on the electrode surface [15]. The catalytic scheme is shown in Fig. 1b. The current on the Tyr-Fe_3O_4@$mSiO_2$/MGCE was much higher than that on the Tyr-Fe_3O_4@SiO_2/MGCE. The increase of the current response was assumed to be attributed to two possibilities. Firstly, although the mesopores cannot be used for Tyr immobilization, they may actually adsorb small molecules [25], phenol in this case, which could facilitate the enzymatic reaction. In addition, the porous structure increases the surface roughness, which facilitates the immobilization of enzyme by increasing amount and better maintaining the enzyme activity.

In addition, the magnetic loading protocol could avoid any additional adhesive, thus decrease the substrate diffusion limitation and increase the sensitivity. For comparison, a (Tyr-Fe_3O_4@$mSiO_2$)-PVA/GMCE was fabricated by adding small amount of adhesive reagent PVA into the Tyr-Fe_3O_4@$mSiO_2$ suspension. As shown in Fig. 4b, similar background currents were observed on (Tyr-Fe_3O_4@$mSiO_2$)-PVA/GMCE and Tyr-Fe_3O_4@$mSiO_2$/GMCE in PBS. However, upon the addition of 50 μM phenol, the reduction peak current with PVA coating significantly decreased. Given the fact of the same amount of enzyme immobilized, the current decrease was mainly attributed to the diffusion limitation generated by the polymer film. The influence by the adhesive was further confirmed by the FIA response. As shown in Fig. 4c, the FIA amperometric response of the Tyr-Fe_3O_4@$mSiO_2$/GMCE to 10 μM phenol at −0.15 V was 7.94 μA, which was about 4.4 times larger than that obtained at the (Tyr-Fe_3O_4@$mSiO_2$)-PVA/GMCE. In addition, the response time after the coating of PVA film was about 2.5 times longer than that without the addition of PVA. All these results indicated the magnetic loading protocol could provide an effective way for the bio-interface fabrication.

Fig. 5a shows the CVs of the Tyr-Fe_3O_4@$mSiO_2$/MGCE in pH 6.0 PBS solution containing 50 μM phenol at different scan rates. The CVs all exhibit peak shaped catalytic waves. With the increase of the scan rate, the peak current increased, and the peak potential shifted negatively. The peak current was proportional to the square of the scan rate ($y = 0.195x + 4.25$, $R^2 = 0.994$), indicating a typical mass diffusion controlled process, which may because of the relative low O_2 content around the Tyr. To confirm this assumption, an O_2 saturated PBS was used to investigate the Tyr catalytic reaction. As shown in Fig. 5b, after 50 μM of phenol was added in the system, a plateau shaped catalytic wave was observed. This phenomenon indicated the kinetic process would be under the control of enzymatic process other than a substrate diffusion process in buffer with saturated O_2.

3.3. Optimization of conditions for biosensor fabrication and phenol detection

To obtain the best performance, several variables including the amount of Tyr-Fe_3O_4@$mSiO_2$ on the electrode surface, the solution pH value, and the potential condition for phenol detection

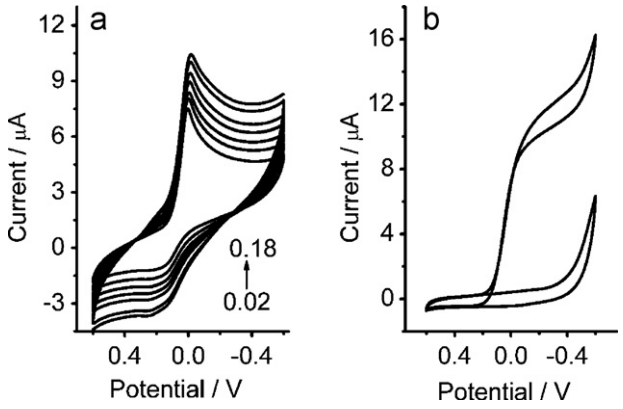

Fig. 5. (a) CVs of the Tyr-Fe_3O_4@$mSiO_2$/MGCE in air saturated pH 6.0 PBS containing 50 μM phenol at scan rate from 20 mV s^{-1} to 180 mV s^{-1} (from lower to higher). (b) The CVs of the Tyr-Fe_3O_4@$mSiO_2$/MGCE in O_2 saturated pH 6.0 PBS with and without the addition of 50 μM phenol at 50 mV s^{-1}.

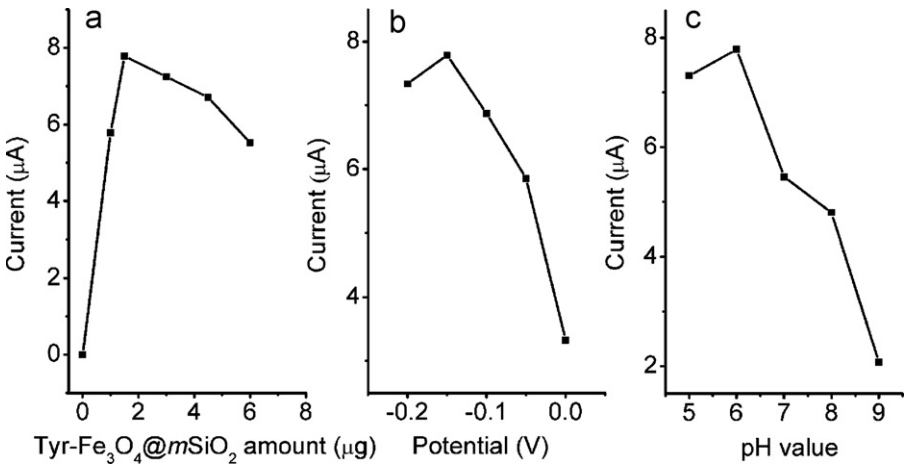

Fig. 6. Influence of the Tyr-Fe_3O_4@$mSiO_2$ modified amount (a), pH value (b), and the detection potential (c) on the FIA response of the Tyr-Fe_3O_4@$mSiO_2$/MGCE to 10 μM phenol 0.1 M PBS at other optimal conditions.

were optimized. When optimizing one variable, other variables were at their optimal values. Fig. 6a shows the effect of the Tyr-Fe_3O_4@$mSiO_2$ amount on the biosensor responses to 10 μM phenol. The best response was obtained at the Tyr-Fe_3O_4@$mSiO_2$ amount of 1.5 μg. Further increasing the amount of enzyme loaded magnetic nanomaterial, the amperometric response decreased. This phenomenon indicated that too much Tyr-Fe_3O_4@$mSiO_2$ was not beneficial for an electrode response due to the diffusion barrier. Therefore, 1.5 μg Tyr-Fe_3O_4@$mSiO_2$ was chosen for the fabrication of biosensor.

The effect of pH on the biosensor response was investigated over a pH range of 5.0–8.0 (Fig. 6b). The maximum response was obtained at pH 6.0, which was in good accordance with other results for Tyr-based biosensors [26–28], and close to that of the free Tyr from mushroom (pH 6.2) [29]. This indicated that the immobilization procedure did not alter the optimum pH of Tyr. Therefore, 0.1 M pH 6.0 PBS was used as the electrolyte in subsequent experiments.

The dependence of the proposed biosensor on the applied potential was displayed in Fig. 6c. The amperometric response increased rapidly with the decreasing potential from 0 to −0.15 V. Afterward, a small decrease of the response was observed, which might be attributed to an increase in the direct reduction of oxygen at the electrode surface, leading to the oxygen depletion within the coating and hence to a decrease in the enzymatic rate [26]. Thus, −0.15 V was selected as the applied potential.

The influence of flow rate was also considered. High flow rate led to a fast response. However, too high flow rate would result in the decrease of the current response and the detaching of the magnetic film. Considering all these factors, 2.0 mL min^{-1} was chosen for the following detection.

3.4. Biosensing application of the Tyr-Fe_3O_4@$mSiO_2$ modified electrode

Under optimal conditions, the biosensor was used for the analysis of phenol. Fig. 7 shows the FIA response of the electrode to successive additions of phenol with the marked concentration. After the addition of phenol, the cathodic current immediately increased and reached 95% of steady-state current within 5 s. The linear range spanned the 4-order concentration of phenol from 1.0×10^{-9} to 1.0×10^{-5} M ($R = 0.999$) with the sensitivity of 78 μA mM^{-1} (1.1 A M^{-1} cm^{-2}) and the detection limit of 1.0 nM. The sensitivity was much higher than the reported 54.2 μA M^{-1} on the $MgFe_2O_4/SiO_2$ [15] modified electrode, 40.76 μA mM^{-1} on the tyrosinase immobilized ZnO Nanorods modified electrode [30], 41.36 mA M^{-1} cm^{-2} on the polyacrylamide polymer modified electrode [31], 0.512 A M^{-1} cm^{-2} on the Fe_3O_4/chitosan modified electrode [7], and 0.030 nA μM^{-1} on the carbon ceramic electrodes [32]. These phenomena could be induced by that the uncovered Fe_3O_4@$mSiO_2$ microspheres with porous structure is propitious to both phenol concentration and Tyr immobilization, and the immobilized Tyr molecules with good bioactivity and concentrated phenol around could lead to a more effective and faster biocatalysis.

The selectivity of the biosensor was evaluated by detecting 10 μM phenol in the presence of the possible interference substrate. In detail, the influences of uric acid of 10 μM, and carbonate, chloride, sulfate, bromide and iodide with concentration of 1.0 mM were investigated. The results showed that these substances did not cause any observable interference in the determination of phenol.

3.5. Stability, reproducibility and real sample analysis

The reproducibility was ascertained by monitoring the current response for 7 replicate injections of 10 μM phenol (Fig. 7) with a relative standard deviation (R.S.D) of 1.5%. The inter-assay precision was estimated at six different electrodes for the determinations in 10 μM phenol. The R.S.D. of inter-assay was found to be 7.1%. The storage stability was determined by storing the phenol biosensor at 4 °C under dry condition. After a storage period of 1 month the biosensor kept 87% of its initial response. Thus, the biosensor showed acceptable reproducibility and stability. Moreover, the renewal of the biosensor interface could be easily achieved by putting a stronger magnet below the electrode, thus avoided any polishing or other serious treatment.

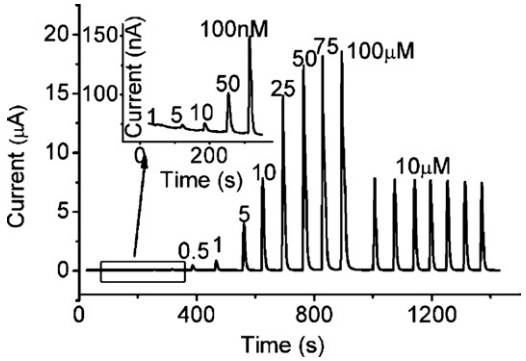

Fig. 7. Flow injection amperometric response of the Tyr-Fe_3O_4@$mSiO_2$/MGCE to the addition of phenol solutions with marked concentration.

Table 1
Recovery studies of phenol in filtered sea water (each result was estimated by three determinations).

Sample	Taken (nM)	Found (nM)	Recovery (%)	RSD (%)
1	2200	2330	106	2.32
2	500	534	107	3.50
3	120	126	106	3.58
4	10	11.1	111	3.91
5	1.2	1.26	105	5.00

To further demonstrate the practicality of the proposed biosensor, the recovery test was studied by adding different amounts of phenol into the filtered sea water. Results were summarized in Table 1. The recoveries were from 105% to 111%. The results indicated that the proposed method was highly accurate and reproducible. It could be used for direct analysis of relevant samples.

4. Conclusion

Fe_3O_4@*m*SiO_2, a magnetic mesoporous microsphere, was successfully used for the construction of magnetic loaded biosensor with magnetic field. The porous and biocompatible surface is beneficial for the loading of Tyr with good bioactivity, hence contributes to the improvement of the sensitivity. The good magnetism provides strong interaction for the nanocomposites to adhere on the magnetic support surface, avoids the addition of any adhesive reagent. Therefore, the adsorbed Tyr molecules could expose entirely in the solution and lead to better affinity to phenol, and a more effective and faster biocatalysis. The biosensor showed several advantages such as fast response, wide linear range, high sensitivity, low detection limit, good reproducibility and stability. The combination of good magnetism with porous structure of Fe_3O_4@*m*SiO_2 shows a great potential for multiple application in electrically active devices.

Acknowledgements

The authors gratefully acknowledge the financial support of the National Natural Science Foundation of China (Nos. 20805003and 20903018), the Research Fund for the Doctoral Program of Higher Education of China (No. 200801411106), and the Young Teachers' Training Foundation (893383) of Dalian University.

References

[1] Y.C. Fu, P.H. Li, Q.J. Xie, X.H. Xu, L.H. Lei, C. Chen, C. Zou, W.F. Deng, S.Z. Yao, Adv. Funct. Mater. (2009) 1784–1791.
[2] Y.C. Fu, C. Chen, Q.J. Xie, X.H. Xu, C. Zou, Q.M. Zhou, L. Tan, H. Tang, Y.Y. Zhang, S.Z. Yao, Anal. Chem. 80 (2008) 5829–5838.
[3] V. Vamvakaki, M. Hatzimarinaki, N. Chaniotakis, Anal. Chem. 80 (2008) 5970–5975.
[4] P. Oennerfjord, J. Emners, G. Marko-Varga, L. Gorton, F. Ortega, E. Dominguez, Biosens. Bioelectron. 10 (1995) 607–619.
[5] J. Zhang, J.P. Lei, Y.Y. Liu, J.W. Zhao, H.X. Ju, Biosens. Bioelectron. 24 (2009) 1858–1863.
[6] Y.C. Zhang, Anal. Chem. 82 (2010) 5275–5281.
[7] S.F. Wang, Y.M. Tan, D.M. Zhao, G.D. Liu, Biosens. Bioelectron. 23 (2008) 1781–1787.
[8] D. Du, M.H. Wang, Y.H. Qin, Y.H. Lin, J. Mater. Chem. 20 (2010) 1532–1537.
[9] Q.F. Luan, J. Li, X. Yao, Electroanalysis 21 (2009) 1799–1804.
[10] Y.Y. Sun, H.Y. Wang, C.Q. Sun, Biosens. Bioelectron. 24 (2008) 22–28.
[11] Q. Rui, K. Komori, Y. Tian, H.Q. Liu, Y.P. Luo, Y. Sakai, Anal. Chim. Acta 670 (2010) 57–62.
[12] D. Du, X.X. Ye, J. Cai, J. Liu, A.D. Zhang, Biosens. Bioelectron. 25 (2010) 2503–2508.
[13] S. Qu, F. Huang, G. Chen, S.N. Yu, J.L. Kong, Electrochem. Commun. 9 (2007) 2812–2816.
[14] F. Mavré, M. Bontemps, S. Ammar-Merah, D. Marchal, B. Limoges, Anal. Chem. 79 (2007) 187–194.
[15] Z.M. Liu, Y.L. Liu, H.F. Yang, Y. Yang, G.L. Shen, R.Q. Yu, Anal. Chim. Acta 533 (2005) 3–9.
[16] A. Miyabayashi, B. Mattiasson, Anal. Chim. Acta 213 (1988) 121–130.
[17] D. Yu, B. Blankert, E. Bodoki, S. Bolllo, J.C. Viré, R. Sandulescu, A. Nomura, J.M. Kauffmann, Sens. Actuators B 113 (2006) 749–754.
[18] C. Zou, Y.C. Fu, Q.J. Xie, S.Z. Yao, Biosens. Bioelectron. 25 (2010) 1277–1282.
[19] S. Qu, J. Wang, J.L. Kong, P.Y. Yang, G. Chen, Talanta 71 (2007) 1096–1102.
[20] H. Tian, J.J. Li, Q. Shen, H.L. Wang, Z.P. Hao, L.D. Zou, Q. Hu, J. Hazard. Mater. 171 (2009) 459–464.
[21] S.L. Gai, P.P. Yang, C.X. Li, W.X. Wang, Y.L. Dai, N. Niu, J. Lin, Adv. Funct. Mater. 20 (2010) 1166–1172.
[22] J. Kim, H.S. Kim, N. Lee, Angew. Chem. Int. Ed. 10 (2008) 8438–8441.
[23] J. Lee, D. Lee, E. Oh, J. Kim, Y.-P. Kim, S. Jin, H.-S. Kim, Y. Hwang, J.H. Kwak, J.G. Park, C.H. Shin, J. Kim, T. Hyeon, Angew. Chem. Int. Ed. 44 (2005) 7427–7432.
[24] Y.H. Deng, D.W. Qi, C.H. Deng, X.M. Zhang, D.Y. Zhao, J. Am. Chem. Soc. 130 (2008) 28–31.
[25] S. Wu, L.L. Zhang, L. Qi, S.Y. Tao, X.Q. Lan, Z.G. Liu, C.G. Meng, Biosens. Bioelectron., doi:10.1016/j.bios.2010.11.029.
[26] Y.Y. Liu, J.P. Lei, H.X. Ju, Electroanalysis, doi:10.1002/elan.201000200.
[27] M. Śnchez-Paniagua Lópeza, F. Tamimib, E. López-Cabarcosc, B. López-Ruiza, Biosens. Bioelectron. 24 (2009) 2574–2579.
[28] E. Han, D. Shan, H.G. Xue, S. Cosnier, Biomacromolecules 8 (2007) 971–975.
[29] R. Bru, A. Sanchez-Ferrer, F. Garcia-Carmona, Biotechnol. Bioeng. 34 (1989) 304–308.
[30] B.X. Gu, C.X. Xu, G.P. Zhu, S.Q. Liu, L.Y. Chen, X.S. Li, J. Phys. Chem. B 113 (2009) 377–381.
[31] Y.X. Cheng, Y.J. Liu, J.J. Huang, K. Li, Y.Z. Xian, W. Zhang, L.T. Jin, Electrochim. Acta 54 (2009) 2588–2594.
[32] H. Behzad, A. Rahmati-Panah, S. Shleev, L. Gorton, Electroanalysis 19 (2007) 907–917.